remote sensing

MDPI

Article

In-Orbit Spectral Response Function Correction and Its Impact on Operational Calibration for the Long-Wave Split-Window Infrared Band (12.0 μm) of FY-2G Satellite

Qiang Guo and Xuan Feng *

National Satellite Meteorological Center, China Meteorological Administration, Beijing 100081, China; guoqiang@cma.gov.cn
* Correspondence: fengxuan@cma.gov.cn; Tel.: +86-10-6840-7057

Academic Editors: Dongdong Wang and Prasad S. Thenkabail
Received: 18 April 2017; Accepted: 31 May 2017; Published: 8 June 2017

Abstract: During the early stage of the G satellite of the Fengyun-2 series (FY-2G), severe cold biases up to ~2.3 K occur in its measurements in the 12.0 μm (IR2) band, which demonstrate time- and scene-dependent characteristics. Similar cold biases in water vapor and carbon dioxide absorption bands of other satellites are considered to be caused by either ice contamination (physical method) or spectral response function (SRF) shift (empirical method). Simulations indicate that this cold bias of FY-2G indeed suffers from equivalent SRF shift as a whole towards the longer wavelength direction. To overcome it, a novel approach combining both physical and empirical methods is proposed. With the possible ice thicknesses tested before launch, the ice contamination effect is alleviated, while the shape of the SRF can be modified in a physical way. The remaining unknown factors for cold bias are removed by shifting the convolved SRF with an ice transmittance spectrum. Two parameters, i.e., the ice thickness (5 μm) and the shifted value (+0.15 μm), are estimated by inter-calibration with reference instruments, and the modification coefficient is also calculated (0.9885) for the onboard blackbody calibration. Meanwhile, the updated SRF was released online on 23 March 2016. For the period between July 2015 and December 2016, the monthly biases of the FY-2G IR2 band remain oscillating around zero, the majorities (~89%) of which are within ±1.0 K, while its mean monthly absolute bias is around 0.6 K. Nevertheless, the cold bias phenomenon of the IR2 band no longer exists. The combination method can be referred by other corrections for cold biases.

Keywords: spectral response function (SRF) correction; cold bias; ice contamination

1. Introduction

Radiometric accuracy is critical for space-to-Earth observation aimed at certain quantitative applications, i.e., weather, climate, and environmental monitoring and forecasting. Particularly, for a usual reflective solar or thermal emissive band, the spectral response function (SRF), which restrains the incident radiation within the specified spectrum, is one of the most important radiometric features influencing the radiometric accuracy of space-borne sensors. For an onboard broadband sensor, its SRFs of different bands are commonly measured during the prelaunch tests and finally provided by the instrument vendor. In fact, although the measurement uncertainties of SRFs inevitably exist, it is a general approach to directly utilize the SRFs measured before launch for in-orbit applications. In the last two decades, some hyper-spectral sounders, i.e., the Atmospheric Infrared Sounder (AIRS) on the Aqua satellite and the Infrared Atmospheric Sounding Interferometer (IASI) on the METOP-A satellite, are in operational service successively with perfect spectral, radiometric, and geolocation performances, and they are widely treated as reference sensors, at least for the meteorological community, to inter-calibrate other ones so as to meet the requirements with high confidence, e.g., climate change detection and calibration accuracy validation [1]. Due to their unprecedented hyper-spectral characteristics, it is possible for these reference sensors (i.e., IASI) to qualify SRF differences and related uncertainties to alleviate other sensor (i.e., High-resolution Infrared Radiation Sounders, HIRS) inter-satellite biases [2].

In recent years, more and more onboard sensors, for example the Moderate-resolution Imaging spectra-radiometer (MODIS) on the Terra satellite [3], the Spinning Enhanced Visible and Infrared Imager (SEVIRI) on Meteosat Second Generation (MSG) [4], and the imager on the Geostationary Operational Environmental Satellite (GOES) [5,6], show significant biases (most of them are cold or negative) in radiation, especially for some atmospheric absorption bands, which are apparently scene- and time-dependent. Existing studies indicate that, although the root cause of these phenomena is basically confirmed to be an enormous SRF variation, it is still not conclusive because other physical error sources, such as blackbody emissivity, detector nonlinearity, and SRF out-of-band response, are not totally understood [3]. However, to overcome such an abnormal condition of SRF variation, two feasible solutions, although not mature enough, are proposed for utilization. The first method (the so-called physical method) is based on the principle of SRF variation primarily caused by a buildup of ice condensed on the surfaces of the sensor's cold optics after outgassing from other materials on the satellite, where a transmittance model of ice is convolved with the SRF before launch to generate a composite one to reduce the cold biases on the whole [4]. The second method (the so-called empirical method) assumes that such a cold bias is triggered by an equivalent shift of the SRF, the optimal shifting value of which can be extracted by comparing with some reference sensors (i.e., IASI) to minimize the absolute scene-dependent slope under the framework of the Global Space-based Inter-Calibration System (GSICS) [5,6]. Nevertheless, although the possible SRF shape changes are ignored in the empirical method, the definite effects caused by ice decontamination on the GOES-12 imager calibration have been investigated overall [7].

Fengyun-2 (FY-2) is the first generation geostationary meteorological satellite in China, playing a key role in worldwide meteorological observations, and its best-performing one (FY-2G) so far has been providing service since July 2015. Recently, a novel internal-blackbody calibration (IBBC) is independently developed to accomplish the in-orbit absolute infrared band calibration of its main meteorological payload, i.e., Visible Infrared Spin-Scan Radiometer (VISSR), for the first time in this series of satellites [8]. Compared with these hyper-spectral reference instruments recommended by GSICS, the monthly mean calibration biases of the long-wave infrared band (IR1: 10.8 μm) and water vapor band (IR3: 6.95 μm) are shown to be lower than 1.0 K for FY-2G (for 90% of cases). Unfortunately, the calibration biases of the long-wave split-window infrared band (IR2: 12.0 μm) of FY-2G could be a cold bias as large as −2.3 K, the similar phenomena of which occurred in MSG-1 and GOES-13 [4–6] within the adjacent spectrum (~13.3 μm).

In our study, three main relevant issues are elaborated step by step. Firstly, based on the in-orbit cold bias situation of the FY-2G IR2 band lasting for about half a year since it has been in service, many potential factors influencing the calibration bias are analyzed, where the root cause is eventually confirmed by a series of simulations with different atmospheric profiles, boundary temperatures, and SRFs. Secondly, a novel approach combining both the physical and the empirical methods is proposed to fulfill the in-orbit SRF correction of the FY-2G IR2 band where the possible SRF variations, including the shift as a whole and shape change, are totally taken into account and optimized by inter-calibrating with some reference sensors (i.e., IASI) under the framework of GSICS, where two spectrum radiance measurement datasets from IASI and FY-2G/VISSR, respectively, are compared after a series of processing steps, including temporal and spatial collocations, as well as spectral matching recommended by the GSICS baseline algorithms and, therefore, the relative biases can be extracted accurately. Thirdly, the realistic impacts of SRF correction on the operational IBBC (i.e., modification coefficient parameter for the calibration slope) are analyzed in detail.

A more complete description of the in-orbit SRF correction method for the FY-2G IR2 band and its impact on the operational IBBC is shown in Section 2. Some primary results from before and after SRF correction are compared in Section 3. In the end, brief discussions and conclusions are provided in Sections 4 and 5, respectively.

2. Methods

2.1. Cold Biases of the FY-2G IR2 Band and Its Root Cause Analysis

2.1.1. Cold Biases of FY-2G IR2 Band During Its Early In-Orbit Situation

At present, as one of the main satellites of the FY-2 series, FY-2G has been in operational service since July 2015 when it was located at 105°E. Unfortunately, compared with the IASI recommended by GSICS, the long-wave split-window infrared band (IR2) of FY-2G behaves with a significant cold bias feature, the monthly mean values of which have worsened from its original −0.17 K in July 2015 to its worst case of −2.56 K in December 2015, and then improved gradually to −1.43 K in February 2016. Meanwhile, the main statistical results (i.e., bias, standard deviation (STD), and samples) are listed in Table 1 and the comparison of the calibration bias scatter diagrams of the IR2 band of the FY-2G satellite for two typical cases (July and December of 2015) is also shown in Figure 1.

Table 1. Calibration biases of FY-2G IR2 band (@290 K) between July 2015 and February 2016.

Time	July 2015	August 2015	September 2015	October 2015	November 2015	December 2015	January 2016	February 2016
Bias(K)	−0.17	−0.08	−0.72	−1.22	−1.44	−2.56	−2.26	−1.43
STD(K)	0.42	0.82	0.61	0.45	0.42	0.70	0.87	0.54
Samples	4027	3390	2378	3491	3452	779	3175	1444

[1] During the first ten-day period of December 2015, the onboard blackbody of FY-2G/VISSR was abnormal and the estimated bias is not for the following analysis.

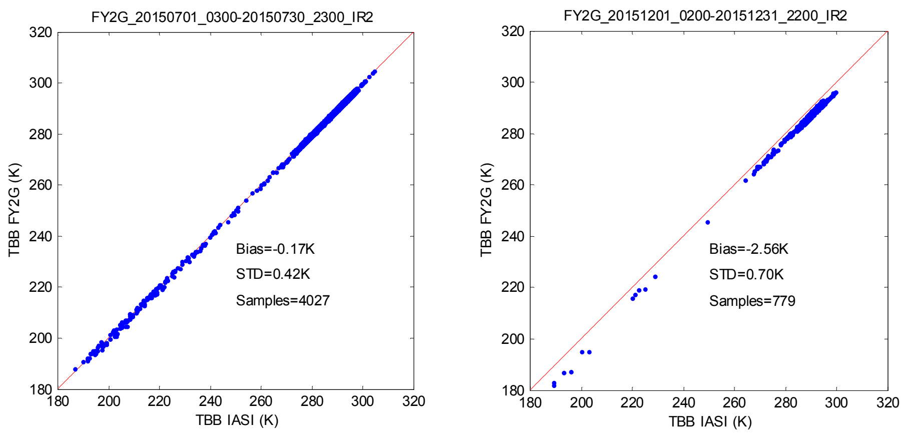

(**a**) (**b**)

Figure 1. Typical scatter diagram comparison of the calibration bias in the IR2 band of the FY-2G satellite from July 2015 to February 2016: (**a**) July 2015, and (**b**) December 2015.

Apparently, during the period between July 2015 and February 2016, the monthly biases of the FY-2G IR2 band are always negative and show time-dependent and periodical characteristics where its maximal value in amplitude occurs in January 2016. At the same time, the monthly STD values of the samples for validation stabilize in the range between 0.42 K and 0.87 K. Due to a short-term abnormal condition of the onboard internal blackbody for the first ten-day period of December 2015, the available samples for validation is relatively smaller than those of other months. Correspondently, during the same period, the monthly biases of the two other infrared bands (IR1 and IR3) of the FY-2G satellite are validated to be less than 1 K for 90% of cases oscillating around zero [8]. Therefore, it actually implies that there is something wrong related with the spectral radiance of the FY-2G IR2 band.

2.1.2. Analysis of Cold Bias for the FY-2G IR2 Band and Identification of Its Root Cause

In real applications, many factors, for example blackbody temperature and emissivity, calibration accuracy of reference instruments, inter-calibration error, nonlinearity, scan mirror emissivity, water ice contamination, and SRF error [5], may influence the validation results of an ordinary infrared band (i.e., IR2). Generally, the above factors can be divided into four different types, whose effects on calibration accuracy are discussed separately, as follows:

- Defects of the Calibration Source

This type of factor includes blackbody temperature and emissivity. On the one hand, the real blackbody temperature is measured from some embedded platinum resistance thermometers (PRTs) and its erroneous temperature measurement will affect all bands (IR1–IR3). Since the cold bias does not occur in IR1 or IR3, blackbody temperature is not likely to be the reason. On the other hand, if such a ~2 K cold bias of the IR2 band is attributed to blackbody emissivity, it would imply its emissivity has been underestimated. Since the emissivity of the IR2 band is accurately measured to be around 0.995, it is unrealistic to suggest that it be larger than unity. Therefore, such types of defects are not the real cause for the cold bias of the IR2 band.

- Defects of Inter-Calibration

For inter-calibration, two factors may affect the validation results of the calibration accuracy of the monitored instrument. The first one is the reference source, i.e., IASI adopted in our study, whose measurement accuracy in the thermal infrared spectra (covering the IR2 band) is estimated to be well within 0.2 K and, therefore, quite stable. Hence, it cannot cause the ~2.3 K cold bias. The second one is the inter-calibration itself. Actually, due to the inevitable collocation errors from both temporal and spatial aspects, as well as the differences in spatial response and viewing geometry for the two sensors during inter-calibration, the validation errors where the random ones dominate the systematic ones are assessed to be ~0.01 K for the typical clear sky condition, but increase rapidly for low radiances by more than one order of magnitude for 210 K scenes [9]. Meanwhile, such a mismatch should affect all bands whilst such a cold bias never occurs for IR1 and IR3 bands of FY-2G. Therefore, it is unlikely that the collocation error and the measurement accuracy of reference instruments are the main causes of the observed cold bias of IR2 band.

- Defects of Instrument Independent of the Spectrum

For all four infrared bands of the FY-2G satellite, the mercury-cadmium-telluride (HgCdTe) detectors are used and calibrated accurately in thermal-vacuum tests before launch. In theory, the nonlinearity response of HgCdTe detectors always exist to varying degrees, particularly for a small incident radiation condition, and is generally dominated by its working temperature [10]. In fact, as indicated in Table 1, the cold bias of the FY-2G IR2 band is not for low-temperature scenes and varies periodically since the working temperature of all infrared detectors remains at 93.5 K during the period between July 2015 and February 2016. Therefore, although the nonlinearity is possibly related with a specific band or dependent of the spectrum, it is also unlikely the main cause of the focused cold bias. On the other hand, it is reported that the scan mirror emissivity which depends on the angle of incidence would lead to a difference of up to ~0.3 K for the similar bands of the GOES imager and MSG-1 SEVIRI without correction [11,12]. Fortunately, due to its spin-stabilized mechanism, the incident angle between the observed target and the normal of FY-2/VISSR main optics remains unchanged for an individual scanning observation, the almost constant background of which can be removed by the onboard space-clamp operation automatically [8]. Clearly, the scan mirror emissivity cannot be the main contributor of the cold bias in the IR2 band.

- Defects of the Instrument Dependent of the Spectrum

As indicated above, a similar cold bias phenomena occurred in some carbon dioxide absorption bands (~13.3 μm) [5,6] as well as some water-vapor absorption bands (~6.5 μm) [3,6] of other instruments, the greatest possible cause of which, supported by the current cognitive ability of the relevant community, is the equivalent SRF shift for a specific band. It should be admitted that it is an empirical explanation and validated by the inter-calibration results against some reference instruments with excellent properties. At the same time, such a resolution is partially proved by the cold bias phenomenon of the MSG-1 SEVIRI 13.4 μm band, the confirmed cause of which is ice contamination, which eventually leads to the variations of both the shape and the central wavelength of its SRF [4].

Figure 2 shows three typical spectral response functions of long-wave infrared bands of different geostationary meteorological satellite instruments, i.e., the FY-2G VISSR IR2 (12.0 μm) band (red), MSG1 SEVIRI 13.4 μm band (blue), and GOES-13 imager 13.3 μm band (green), the latter two available at the website: https://www.star.nesdis.noaa.gov/smcd/GCC/instrInfo-srf.php [13]. Meanwhile, the two ~13 μm bands of MSG1 and GOES-13 cover a stronger carbon dioxide absorption spectra of between 13 μm and 14 μm, which is demonstrated by the clear-sky spectral radiance (black solid line in Figure 2) for the U.S. Standard Atmosphere, and indeed suffers from the severe cold bias effects [5,6]. Regardless of the real causes for the cold bias phenomena of the MSG1 and GOES-13 satellites, they eventually result in the equivalent SRF shift of a specific band compared with some reference instruments (i.e., IASI).

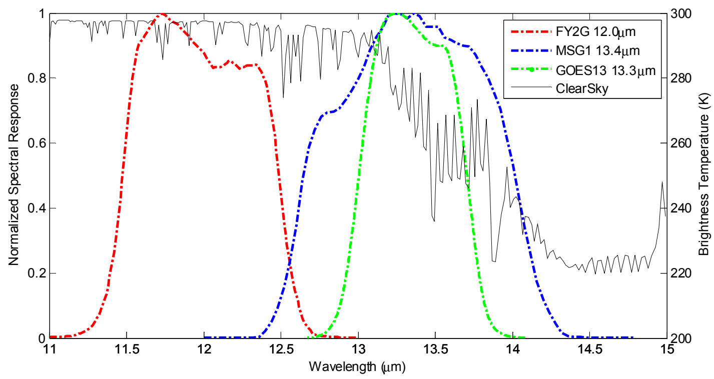

Figure 2. Typical spectral response functions, i.e., red for the FY-2G IR2 (12.0 μm) band, blue for the MSG1 13.4 μm band, green for the GOES-13 13.3 μm band, and clear-sky spectral radiance (presented as brightness temperature) for the U.S. Standard Atmosphere.

Therefore, to validate whether or not the time- and scene-dependent cold bias of the FY-2G IR2 band, which covers some weak water vapor absorption spectra as shown in Figure 2, is related with the shift of its SRF, some simulations are done with six representative atmospheric conditions or models, as well as different possible shifted values (−0.20, −0.15, −0.10, −0.05, 0.05, 0.10, 0.15, 0.20, unit: μm) of its SRF against its normal one. These models are tropical, mid-latitude summer, mid-latitude winter, sub-arctic summer, sub-arctic winter and 1976 U.S. standard ones, respectively, which are widely utilized in moderate-resolution atmospheric transmission (MODTRAN) software, and their humidity and temperature profiles are also shown in Figure 3. In addition, six boundary temperatures, i.e., 250 K, 260 K, 270 K, 280 K, 290 K, and 300 K, are applied in each of the six atmospheric models above, respectively.

Figure 4 illustrates the brightness temperature difference(s) (ΔBT) varying with different shifted value(s) of the FY-2G IR2 band SRF on the different conditions of boundary temperatures for six representative atmospheric models. ΔBT is defined as the measured BT with the shifted SRF subtracted by the one with the original SRF at the same boundary temperature, as well as the same atmospheric model. There is no doubt that ΔBT becomes zero when the shifted value is equal to zero for all of the boundary temperature and atmospheric model conditions. In general, for the six atmospheric models shown in Figure 2, the variation tendencies of ΔBTs are monotonic and basically similar with each other for any selected boundary temperature. Specifically, when the shifted values are negative, ΔBT of a lower boundary temperature (e.g., 250 K) is smaller than that of a higher one (e.g., 300 K), which means that the SRF shift towards the shorter wavelength direction will cause the cold targets colder and the hot ones hotter. However, when the shifted values become positive, ΔBTs vary in the reverse direction against the negatively-shifted situations. Considering that the reference BT of monitored biases for the IR2 band is recommended to be 290 K, it is equivalent to measure the clear-sky scene with its boundary temperature between 290 K and 300 K at least for the six representative atmospheric models for simulation. Apparently, validated by the simulation results from all six atmospheric models, as shown in Figure 4, it is most likely that the shift or equivalent shift of SRF towards the longer wavelength direction (namely the positively-shifted value) is the root cause of cold bias effect for the FY-2G 12.0 μm band at the 290 K reference in BT. Although the definite physics of such an equivalent SRF shift for the FY-2G IR2 band are still unclear, it actually provides a reasonable method to solve the severe cold bias phenomenon based on a number of simulations, at least in the statistical sense. Therefore, the next step is to determine what possible factors can cause the SRF shift and how much the SRF shifts, equivalently.

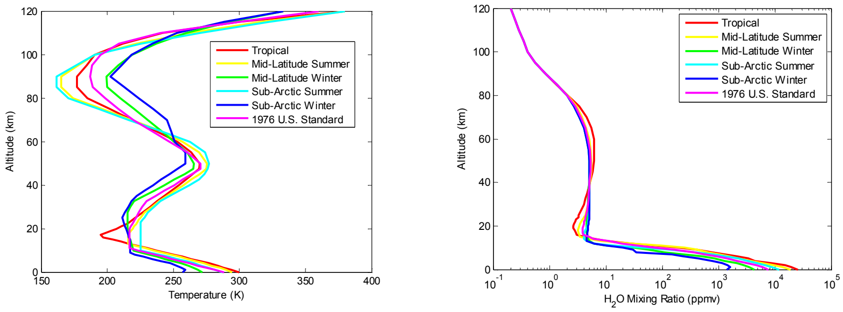

(**a**) (**b**)

Figure 3. Humidity and temperature profiles of six representative atmosphere conditions: (**a**) temperature profiles; and (**b**) humidity profiles.

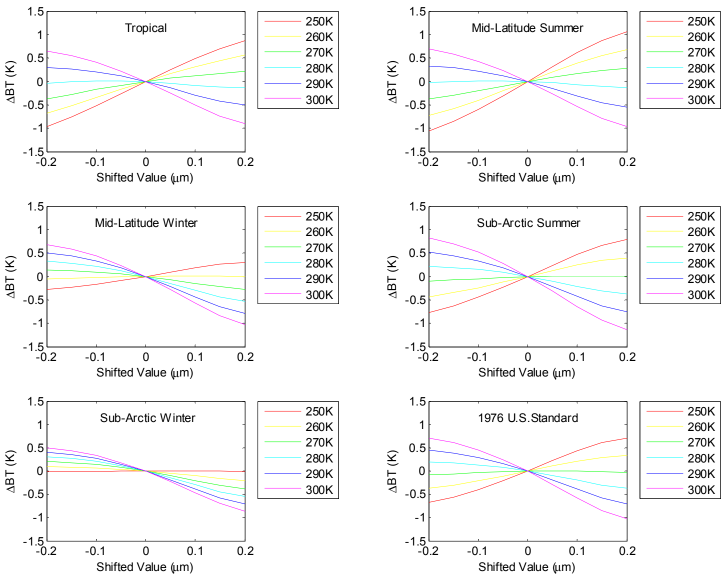

Figure 4. Brightness temperature differences varying with different shifted values of the FY-2G IR2 band SRF on the different conditions of boundary temperatures for six representative atmospheric models.

2.2. A Novel Approach Combining Both Physical and Empirical Methods for In-Orbit SRF Correction

In general, there are a few published studies on in-orbit SRF correction for long-wave infrared bands so far [2–7], the possible cause of which is either the physical ice contamination or empirically regarded as an equivalent SRF shift as a whole. On the one hand, for the FY-2G IR2 band, the inevitable outgassing from other material on the satellite condenses as a buildup of ice film on the surfaces of the cold optics and eventually changes its SRF distribution. On the other hand, since the impacts of ice contamination on Meteosat-8/9 still exist after 5–6 decontamination operations during their mission time [4], the influence of ice contamination on the IR2 band is very likely to occur during the early in-orbit stage of the FY-2G satellite, after only one decontamination operation. Nevertheless, the equivalent SRF shift caused by some uncertain or unknown factors is still to be considered to enhance the final radiometric accuracy of measurements. Therefore, in this article, a novel approach combining both physical and empirical methods (i.e., both the ice contamination and the equivalent SRF shift are taken into account together) is proposed to solve the in-orbit SRF correction of the FY-2G IR2 band, the main sketch of which is illustrated in Figure 5.

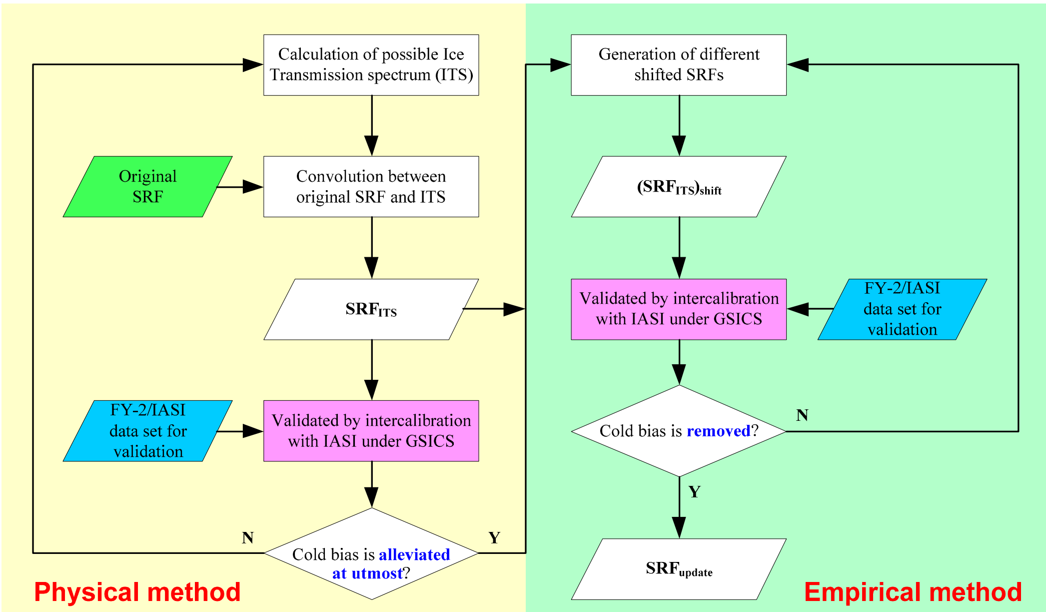

Figure 5. Main sketch of the approach combining both physical and empirical methods for SRF correction of the FY-2G IR2 band.

Specifically, two main components, i.e., the physical method (with the light yellow shadow) and the empirical one (with the light green shadow) in Figure 5, comprise the whole combination approach. For the former, the ice transmission spectrum (ITS), with some possible different ice thicknesses once tested before launch [14], can be calculated by using the discrete ordinates radiative transfer (DISORT) program [15]. Using Mie theory, the three other required input parameters for the DISTORT program, i.e., the absorption efficiency, the scattering efficiency, and the asymmetry factor, can be determined with some given radius of the ice particles, wavelength, as well as the complex refractive index of the medium [16,17]. Then, the SRF affected by ITS ($\mathbf{SRF_{ITS}}$) can be computed by convolution between the original one and the derived ITS, and its impact on the calibration accuracy can be validated by inter-calibration between FY-2G/VISSR and METOP-A/IASI under the framework of GSICS. It should be stated that all of the possible ($\mathbf{SRF_{ITS}}$)s are validated separately, where the best one is determined in the sense of cold bias alleviation and utilized as the input SRF of the empirical method. For the latter, according to the simulation results in Section 2.1, the $\mathbf{SRF_{ITS}}$ is shifted as a whole in the longer wavelength direction by a series of distances on the order of 10^{-2}~10^{-1} μm, individually, to generate a guessed SRF, i.e., $(\mathbf{SRF_{ITS}})_{\mathbf{shift}}$, which is also used for inter-calibration to validate whether or not the cold bias can be removed.

In addition, the determination conditions of physical and empirical methods, i.e., "alleviated at utmost" and "removed" in Figure 5, can be given by the mean bias ($\overline{bias}$), i.e.:

$$\overline{bias} \triangleq \frac{1}{N} \sum_{i \in [1,N]} bias^{i}_{monthly} \Bigg|_{SRF_{ITS}@t_j} \rightarrow \max,\ \overline{bias} < 0, \text{where } t_j \text{ is a possible ice thickness} \tag{1}$$

$$\overline{bias} \triangleq \frac{1}{N} \sum_{i \in [1,N]} bias^{i}_{monthly} \Bigg|_{(SRF_{ITS})_{shift}@d_k} \rightarrow 0^{-},\ \text{where } d_k \text{ is a shifted value of SRF as whole} \tag{2}$$

where i represents the different month-time between July 2015 and February 2016 (except for December 2015) for cold bias analysis in this case and *bias* is the monthly validated result from inter-calibration. It is implied that the SRF correction aimed at ice contamination is merely to alleviate the impact of cold bias as much as possible, given by Equation (1), although the shape of SRF can be modified in a physical way. The rest of the unknown factors for cold bias, however, can be nearly removed (namely $\overline{bias}$ approaches zero from its original negative value, as indicated in Equation (2) by shifting $\mathbf{SRF_{ITS}}$ in an empirical way). At all events, the merit of the eventual radiometric accuracy after SRF correction is to inter-calibrate with some reference instruments.

2.3. Impact of the SRF Correction on the Operational IBBC Approach

In this subsection, the main impact of SRF correction on the in-orbit operational internal-blackbody calibration (IBBC) will be briefly analyzed. Viewing the internal blackbody, the net incident radiance after background restraint ($L_{i,n}$) in band i of FY-2G/VISSR consists of three main components, i.e., the radiances from the internal blackbody ($L_{i,IBB}$), the front optics ($L_{i,FO}$), and the calibration optics ($L_{i,CO}$), and can be given by [8]:

$$L_{i,n} = L_{i,IBB} - L_{i,FO} + L_{i,CO} \tag{3}$$

where the radiometric contribution coefficients of both front and calibration optics are nearly constant and have been accurately measured in prelaunch tests. Then, viewing this internal blackbody with the original SRF ($srf_{i,original}(\lambda)$), the measured radiance ($L_{i,m}$) by the uncorrected instrument is:

$$L_{i,m} = \frac{\int L_{i,n} \cdot srf_{i,original}(\lambda) \cdot d\lambda}{\int srf_{i,original}(\lambda) \cdot d\lambda} \tag{4}$$

When viewing with the corrected SRF ($srf_{i,update}(\lambda)$), the measured radiance ($L'_{i,m}$) for the internal blackbody can be written as:

$$L'_{i,m} = \frac{\int L_{i,n} \cdot srf_{i,update}(\lambda) \cdot d\lambda}{\int srf_{i,update}(\lambda) \cdot d\lambda} \tag{5}$$

Assuming that the radiometric response of FY-2G/VISSR is linear within its dynamic range for each band and almost independent of the incident radiance spectrum, the basic calibration equation for band i is:

$$L_{i,m} = C_{i,1} \cdot v_{i,m} + C_{i,0} \tag{6}$$

$$L'_{i,m} = C_{i,1} \cdot v'_{i,m} + C_{i,0} \tag{7}$$

where $C_{i,1}$ and $C_{i,0}$ are the calibration slope and offset for band i, and $v_{i,m}$ and $v'_{i,m}$ are the measured results in voltage with original and corrected SRFs, respectively. In practice, since $C_{i,0}$ is naturally close to zero, $C_{i,1}$ can be estimated by:

$$C_{i,1} \cong \frac{L_{i,m}}{v_{i,m}} = \frac{L'_{i,m}}{v'_{i,m}} \tag{8}$$

where the estimated value of $C_{i,1}$ is theoretically accurate. Therefore, the outcome of the operational IBBC without SRF correction, particularly the calibration slope ($C_{i,1}^{OP}$), should be modified against the true value ($C_{i,1}$) by a coefficient k, namely:

$$k \hat{=} \frac{C_{i,1}}{C_{i,1}^{OP}} = \frac{L'_{i,m}}{L_{i,m}}, \text{ where } C_{i,1}^{OP} = \frac{L_{i,m}}{v'_{i,m}} \tag{9}$$

Equation (9) provides the modification coefficient (k) to the operational IBBC of the FY-2G/VISSR thermal infrared band (i.e., IR2), which should face SRF correction due to cold biases.

3. Results

In this section, the main results of the SRF correction for the FY-2G IR2 band, including some intermediate ones from both physical and empirical methods as shown in Figure 5, are provided and analyzed in detail. Meanwhile, the validations given by inter-calibration with and without SRF correction, separately, are also illustrated for comparison so as to confirm the eventual performance of the proposed combined approach.

3.1. Results of the Physical Method under Some Limited Conditions

Figure 6 shows some possible SRF variations of FY-2G IR2 band caused by ice contamination to varying degrees. Specifically, Figure 6a shows a series of ITSs calculated with various possible ice-layer thicknesses from 1.0 to 5.0 μm once measured in prelaunch tests under different decontamination operations [14] where the upper bound value of 5.0 μm should be modified for different satellites, and the corresponding (**SRF$_{\mathbf{ITS}}$**)s are generated by convolution between the original one (in the black dashed line) and ITSs in Figure 6b. Although a strong absorption peak of thin film ice occurs around 11.9 μm for all tof he thickness conditions, the shapes of the convolved SRFs show significant difference against the original one merely within the range between 12.0 and 12.5 μm.

Table 2 illustrates the statistical results of different (**SRF$_{\mathbf{ITS}}$**) impact on its equivalent central wavelength, as well as the mean bias ($\overline{bias}$) defined in Equation (1) calculated with the measurements from July 2015 to February 2016 (except for December 2015) of the FY-2G satellite. It is clear that (**SRF$_{\mathbf{ITS}}$**) convolved by ITS with different ice-layer thicknesses can cause its equivalent central wavelength to move towards the longer wavelength direction from its original 11.967 μm to 11.979 μm gradually, which alleviates the cold bias influences by 0.01 to 0.06 K, respectively, despite its limited effects against the remaining mean bias of calibration around −1 K. According to the principle given by Equation (1), the (**SRF$_{\mathbf{ITS}}$**) with a 5 μm ice layer is confirmed to be the best choice for the physical method.

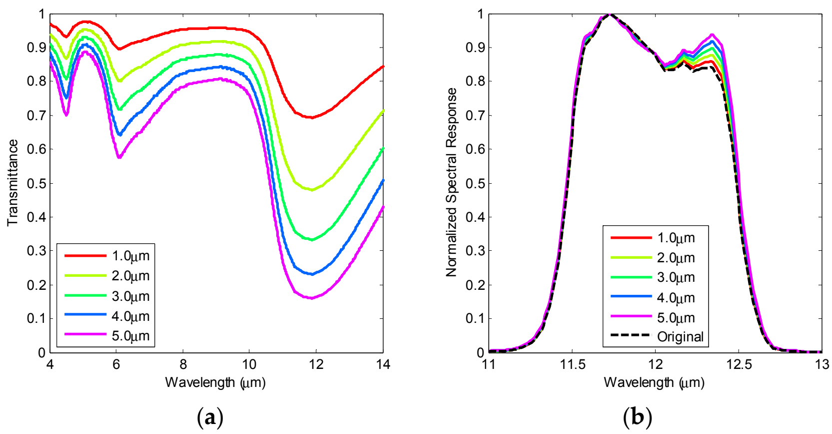

Figure 6. SRF variations of the FY-2G IR2 band caused by ice contamination with possible ice-layer characteristics. (**a**) ITS with different ice-layer thickness; and (**b**) convolved SRFs with different ITSs.

Table 2. Statistical results of $\mathbf{SRF_{ITS}}$ impact on the central wavelength and bias of the FY-2G IR2 band.

	$\mathbf{SRF_{original}}$	$\mathbf{SRF_{ITS}}$ **@Different Ice Layer Thickness (μm)**				
		1.0	**2.0**	**3.0**	**4.0**	**5.0**
Central wavelength (μm)	11.967	11.970	11.972	11.974	11.977	11.979
$\overline{bias}$ (K)@290 K	−1.05	−1.04	−1.03	−1.02	−1.01	−0.99

Based on the above-analyzed results, although the in-orbit ice contamination caused by the outgassing from other materials on the satellite is inevitable, its impact on the cold bias effect of the FY-2G IR2 band is positive, but minor. Nevertheless, it provides a feasible method to modify the shape of the SRF in a physical way and should be applied to correct the SRF ahead of the empirical method.

3.2. Results of the Empirical Method for an Optimal SRF-Shift Estimation

As indicated in Figure 5, the empirical method can be implemented through shifting $\mathbf{SRF_{ITS:\,5\mu m}}$ by a positive distance in wavelength, whose impacts on the radiometric accuracy are provided by the inter-calibration between FY-2G/VISSR and METOP-A/IASI with the collocated measurements during the period between July 2015 and February 2016 (except for December 2015) under the framework of GSICS. As given by Equation (2), when the mean bias ($\overline{bias}$) approaches zero as closely as possible (but still remains negative), the shifted value of $\mathbf{SRF_{ITS:\,5\mu m}}$ is the demanded one for the empirical method. Figure 7 shows the evaluated monthly biases of the FY-2G IR2 band with some possible shifted values of $\mathbf{SRF_{ITS:\,5\mu m}}$ against those of its original one. It is known that the cold bias effects can be alleviated by shifting SRF as a whole towards the longer wavelength direction whilst $\overline{bias}$ approaches zero gradually. In particular, when the shifted values are +0.14 μm, +0.15 μm, and +0.16 μm in Figure 7, the corresponding $\overline{bias}$ values are validated to be −0.09 K, −0.04 K, and 0.01 K, respectively. Therefore, according to the principle given by Equation (2), the shifted value of +0.15 μm is the optimized one for the empirical method, where the monthly bias distribution of the FY-2G IR2 band is almost unbiased.

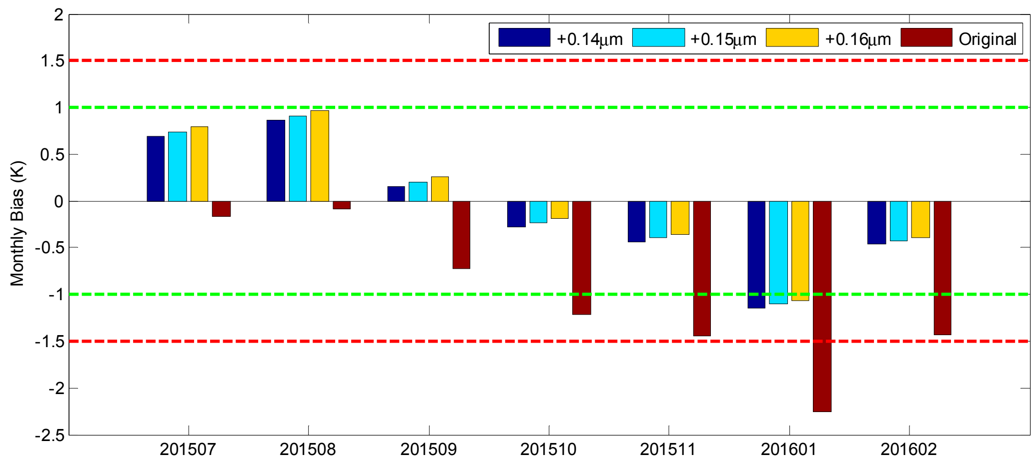

Figure 7. Monthly biases of the FY-2G IR2 band with different shifted values of $\mathbf{SRF_{ITS:\,5\mu m}}$ against those of its original one.

3.3. Long-Term Monthly Biases of FY-2G IR2 Band Monitored under GSICS

Based on the analyzed results from the proposed combined approach, the causes of the cold bias of the FY-2G IR2 band consists of two aspects, i.e., a 5 μm-ice-layer contamination, as well as an equivalent SRF shift as a whole by +0.15 μm, and the final updated SRF for users are shown against its original one in Figure 8. The updated spectral characterization data of the FY-2G IR2 (12.0 μm) band was released at the website: http://www.nsmc.org.cn/en/NSMC/Contents/100157.html [18] on 23 March 2016, where its shape is generally similar to that of the predecessor, except for a certain enhancement near the after-edge of SRF, itself, and its central wavelength is eventually shifted by about +0.162 μm. Meanwhile, the modification coefficient (k) given by Equation (9) for the FY-2G IR2 band is calculated to be 0.9885 and has been updated in the operational IBBC software.

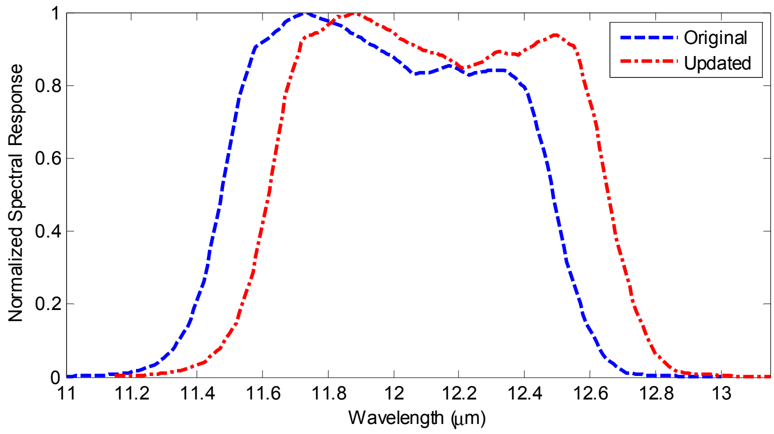

Figure 8. The original and updated SRFs of the FY-2G IR2 (12.0 μm) band.

To validate the real performance of the combination methods for cold bias restraint, the updated SRF of the FY-2G IR2 (12.0 μm) band, together with the original ones of other thermal infrared bands, i.e., IR1 (10.8 μm) and IR3 (6.95 μm), are utilized for inter-calibration with METOP-A/IASI for the period between July 2015 and December 2016, the results of which are shown in Figure 9. It is indicated that the monthly biases for the three bands of FY-2G remain oscillating around zero, the majorities (~89%, except for in December 2015, when the onboard blackbody operation was abnormal) of which are generally within ±1.0 K. During this analysis period, the mean monthly absolute biases of the three infrared bands (i.e., IR1–IR3) are around 0.42 K, 0.61 K, and 0.56 K, respectively. Similar to those in both IR1 and IR3 bands, the significant cold bias phenomenon of IR2 has no longer existed since March, 2016. This implies that, at least for the current condition, only the IR2 band needs the in-orbit SRF correction to achieve the reasonable calibration performance, in general, for the FY-2G satellite, as shown in Figure 9.

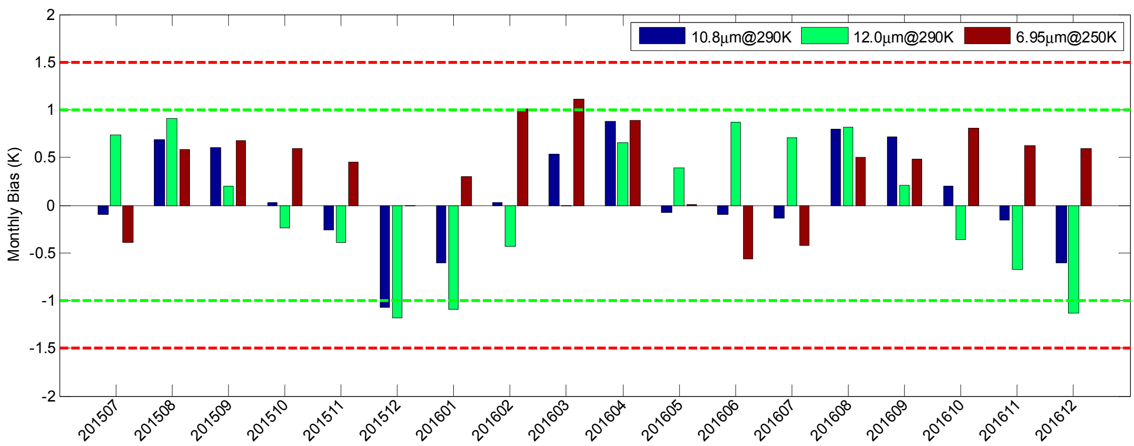

Figure 9. Monthly biases of main infrared bands of FY-2G/VISSR satellite between July 2015 and December 2016 against METOP-A/IASI.

4. Discussion

Cold bias once occurs in the measurements from some broad water vapor absorption (~6.5 μm) and carbon dioxide absorption (~13.3 μm) bands of Terra/MODIS, MSG-1/SEVIRI, and GOES-13/imager. There are two available solutions for such a cold bias. The first one is called the physical method, which deals with the SRF variation caused by the thin ice-layer condensed on the surfaces of cooled optics and is applied in the SRF correction of the MSG-1/SEVIRI 13.3 μm band. Recently, work done on Landsat-5 ice decontamination with a multiple-ice-layer thickness model has been validated to increase the calibration accuracy and is expected to benefit the proposed combination methods in the near future. The second one is called the empirical method, where the SRF shift as a whole is simply considered the root cause and the shifted value can also be estimated by the inter-calibration with some reference instrument (i.e., IASI). The empirical method is also adopted in some infrared bands of GOES imagers. However, the deficiencies of the two methods are evident. For the former, although it can modify the shape of SRF in a physical way, it cannot overcome the cold bias effects occurring in the similar bands of GOES satellite [5]. For the latter, regardless of the possible shape variations of SRF, only its whole shift towards the longer wavelength direction is taken into account. Apparently, the main considerations of the proposed combination methods are to utilize the physical method (generating the convolved $\mathbf{SRF_{ITS}}$ from the condensed ice film) and the empirical method (generating the shifted SRF as a whole) in an orderly manner. Meanwhile, aiming at some other possible contamination sources (i.e., silicon film found in other onboard sensors), the basic processing steps of the physical method are also suitable.

Theoretically, it is an optimal and accurate manner to measure the SRF characteristics of a sensor's specified bands before launch and keep it as unchanged as possible, although it is definitely difficult under in-orbit conditions. Moreover, it should be emphasized that all of the physical, empirical, as well as the proposed combination methods are acceptable solutions in statistics under the framework of intercalibration (i.e., GSICS) to achieve the more identical data quality compared with some reference sensor (i.e., IASI).

In practice, when a certain (warm or cold) bias dependent of real scenes appear in the measured radiance or BT, the root cause is usually its SRF variation, which can be mitigated by some SRF correction operation, e.g., the proposed combination methods. Therefore, since the monthly averaged biases of IR1 and IR3 bands of the FY-2G satellite oscillate around zero after launch, there is no need to correct their SRFs at all.

5. Conclusions

In this article, considering that the measurements of the FY-2G IR2 band embody representative cold bias characteristics (i.e., time- and scene-dependence) and the ice contamination due to the outgassing from other materials of the satellite is inevitable, the approach combining both physical and empirical methods for in-orbit SRF correction is proposed. On the one hand, based on the possible ice thicknesses once tested before launch, the ice contamination effect is compensated by the modification of the shape of the SRF in a physical way. On the other hand, the remaining unknown factors for cold bias are removed by shifting the convolved SRF ($\mathbf{SRF_{ITS}}$) as a whole. It should be stated that the ice thickness (5 μm) and the shifted value (+0.15 μm) are estimated by inter-calibration under GSICS. Meanwhile, the modification coefficient is also deduced and calculated (0.9885) for the operational IBBC application.

In summary, although the actual mechanism of cold bias phenomena is not exactly known, the proposed combined approach is more integrated and validated by the utilization in SRF corrections of the FY-2G IR2 band, and can be referred by other corrections for cold biases.

Acknowledgments: The authors wish to thank Gui-Lin Chen and Yun-Tian Pei of Shanghai Institute Technical Physics (SITP), Chinese Academy of Sciences (CAS), for providing the testing results of FY-2/VISSR before launch. The authors also wish to express their gratitude to Jian-min Xu and Zhi-qing Zhang of National Satellite

Meteorological Center (NSMC) for their insightful discussions and advice on this research. This paper was supported by the National Natural Science Foundation of China under grant Nos. 41275034 and 91338203.

Author Contributions: Qiang Guo is the main author of this research work and wrote the manuscript. Xuan Feng developed the transmittance computation codes due to ice contamination, as well as parts of the spectral matching codes for intercalibration between FY-2G/VISSR and IASI. Both the authors reviewed and edited the manuscript.

Conflicts of Interest: The authors declare no conflict of interest.

References

1. Goldberg, M.; Ohring, G.; Butler, J.; Cao, C.; Datla, R.; Doelling, D.; Gartner, V.; Hewison, T.; Iacovazzi, B.; Kim, D.; et al. The global space-based inter-calibration system. *Bull. Am. Meteorol. Soc.* **2011**, *92*, 467–475. [CrossRef]
2. Cao, C.; Goldberg, M.; Wang, L. Spectral bias estimation of historical HIRS using IASI observations for improved fundamental climate data records. *J. Atmos. Ocean. Technol.* **2009**, *26*, 1378–1387. [CrossRef]
3. Sohn, B.J.; Kim, B.R.; Lee, S.S. Possible shift of spectral response function of the MODIS 6.8 µm water vapor channel causing a cold bias up to 3 K. *Atmos. Meas. Tech.* **2010**, *3*, 1667–1672. [CrossRef]
4. Hewison, T.J.; Müller, J. Ice Contamination of Meteosat/SEVIRI Implied by Intercalibration against Metop/IASI. *IEEE Trans. Geosci. Remote Sens.* **2013**, *51*, 1182–1186. [CrossRef]
5. Wu, X.; Yu, F. Correction for GOES Imager Spectral Response Function Using GSICS. Part I: Theory. *IEEE Trans. Geosci. Remote Sens.* **2013**, *51*, 1215–1223. [CrossRef]
6. Yu, F.; Wu, X. Correction for GOES Imager Spectral Response Function Using GSICS. Part II: Applications. *IEEE Trans. Geosci. Remote Sens.* **2013**, *51*, 1200–1214. [CrossRef]
7. Wang, L.; Wu, X.; Weng, F.; Goldberg, M.D. Effects on Ice Decontamination on GOES-12 Imager Calibration. *IEEE Trans. Geosci. Remote Sens.* **2013**, *51*, 1224–1230. [CrossRef]
8. Guo, Q.; Chen, F.; Chen, B.; Feng, X.; Yang, C.; Wang, X.; Zhang, Z. Internal-blackbody calibration (IBBC) approach and its operational application in FY-2 meteorological satellites. *Quart. J. R. Meteorol. Soc.* **2016**, *142*, 3082–3096. [CrossRef]
9. Hewison, T.J. An Evaluation of the Uncertainty of the GSICSSEVIRI-IASI Intercalibration Products. *IEEE Trans. Geosci. Remote Sens.* **2013**, *51*, 1171–1181. [CrossRef]
10. Norton, P. HgCdTe Infrared Detectors. *Opto-Electron. Rev.* **2002**, *10*, 159–174.
11. Weinreb, M.P.; Jamieson, M.; Fulton, N.; Chen, Y.; Johnson, J.X.; Smith, C.; Bremer, J.; Baucom, J. Operational calibration of GOES-8 and -9Imagers and Sounders. *Appl. Opt.* **1997**, *36*, 6895–6904. [CrossRef] [PubMed]
12. Van de Berg, L.; Heinemann, T.; Szyndel, M.; von Bremen, L.; König, M.; Rogers, C.; Pili, P.; Yildrim, A. The Calibration of the infrared channels of Meteosat first and second generation spacecraft. In Proceedings of the EUMETSAT Meteorological Satellite Conference, Weimar, Germany, 29 September–3 October 2003.
13. Spectral Response Functions. Available online: https://www.star.nesdis.noaa.gov/smcd/GCC/instrInfo-srf.php (accessed on 6 June 2017).
14. Guo, Q.; Pei, Y.; Lan, Z. Study of H_2O Contamination on a Cooled Optical Surface. *J. Infrared Millimeter Waves* **1995**, *14*, 132–138.
15. Stamnes, K.; Tsay, S.; Wiscombe, W.; Jayaweera, K. Numerically stable algorithm for discrete-ordinate-method radiative transfer in multiple scattering and emitting layered media. *Appl. Opt.* **1988**, *27*, 2502–2509. [CrossRef] [PubMed]
16. Gardner, A.S.; Sharp, M.J. A review of snow and ice albedo and the development of a new physically based broadband albedo parameterization. *J. Geophys. Res.* **2010**, *115*, F01009. [CrossRef]
17. Warren, S.G.; Brandt, R.E. Optical constants of ice from the ultraviolet to the microwave: A revised compilation. *J. Geophys. Res.* **2008**, *113*, D14220. [CrossRef]
18. Notice about Update of SRF for FY-2G Infrared Channel 2. Available online: http://www.nsmc.org.cn/en/NSMC/Contents/100157.html (accessed on 6 June 2017).